

Segmentation and Tracking of Myocardial Boundaries Using Dynamic Programming

Athira J. Jacob, Varghese Alex, and Ganapathy Krishnamurthi^(✉)

Indian Institute of Technology-Madras, Chennai, India
gankrish@iitm.ac.in

Abstract. Increasing interest in quantification of local myocardial properties throughout the cardiac cycle from tagged MR (tMR) calls for treatment of the cardiac segmentation problem as a spatio-temporal task. The method presented for myocardial segmentation, uses dynamic programming to choose the optimal contour from a set of possible contours subject to maximizing a cost function. Robust Principle Component Analysis (RPCA) is used to decompose the time series into low rank and sparse components and initialization of the contour is done on the low rank approximation. The 3D nature of the images and tag grid location is incorporated into the cost function to get more robust results. 3D+t segmentation of patient data is achieved by propagating contours spatially and temporally. The method is ideal as a pre-processing step in motion quantification and strain rate mapping algorithms.

Keywords: Dynamic programming · Tagged MR image analysis · Robust PCA · Deformable contours · Tracking · 4D cardiac images · Tag

1 Introduction

Currently cardio-vascular magnetic resonance (MR) is the gold standard for assessing global as well as regional heart function due to its high spatial and temporal resolution [2]. In 1988, Zerhouni et al. [9] introduced a MR based non-invasive method for imaging called tagged MRI. Since then tagged MR techniques have shown great potential for noninvasively measuring local mechanical wall function. Segmentation and tracking of the heart wall boundaries and tags is an important step in tMR image analyses tasks. There has been some amount of research efforts on the automated myocardial contour segmentation. Many rely on suppression or removal of tags before segmentation [3, 4, 8]. Active shape models have been used with learning based methods [6]. Segmentation of tagged MR images still remains a difficult task due to the common presence of cluttered objects, complex object textures, image noise, intensity inhomogeneity, and especially the complexities added by the tagging lines.

We have devised a flexible, fast, non-iterative algorithm that exploits intensity and geometrical priors intrinsic to the image task. It uses Dynamic Programming (DP) to localize the contours and propagate them through subsequent

spatial and temporal frames. The key contributions of this paper are highlighted as follows

1. Novel use of Stable Principle Components Pursuit (SPCP), a variation of RPCA, to obtain a low rank approximation which is used to automatically obtain initial contour.
2. A robust and effective segmentation framework for segmenting myocardial boundaries in tagged MR images that exploits tag information, which is usually neglected or not well exploited. The method also exploits intensity and geometric information inherent to the images.
3. The spatio-temporal approach of the algorithm makes it suitable to be used along with deformation mapping algorithms of the myocardial tissue.

2 Data

The data used hosted by the Cardiac Atlas Project, originally for the Motion tracking challenge in 2011 [7], consists of 15 scans of healthy volunteers. Each volunteer case consists of cardiac MRI and 3D ultrasound images. The MR acquisition includes: (1) cine SSFP sequences in 2-chamber, 4-chamber, and short-axis views, (2) a whole-heart SSFP sequence gated at end-diastole and end-expiration; and (3) a 4D tMR sequence. The tMR volumes are of size $112 \times 112 \times 111$ (in pixels) with a resolution of 1 mm/pixel and around 25 volumes per cardiac cycle. Tagging is present in three orthogonal directions.

3 Method

Firstly, RPCA and intensity based thresholding is used to initialize a rough endocardium border, which is fit into a circle and sampled to get an initial list of candidate points for endocardium. Using sample points from a circular contour introduces an implicit shape prior and incorporates robustness against missing edges and non-myocardial structures. Each point is used to define a search list around it and DP is used to select one point from each search list by minimizing a cost function. Both geometry and intensity information from the 3D volume is used to define the cost function. The identified endocardial boundary is then used to initialize a rough epicardial boundary and the algorithm proceeds as before except for a change in the cost function. The contours are then propagated spatially and temporally. Apart from traditional applications, this method is particularly suitable for elastography, strain and strain rate imaging etc. to delineate myocardial tissue as the region of interest. The entire procedure of our framework is demonstrated in Fig. 1.

3.1 Robust Principle Component Analyses

Robust PCA (RPCA) [1] is a technique that decomposes a given matrix into a low-rank component and sparse component. In this paper, we have used the

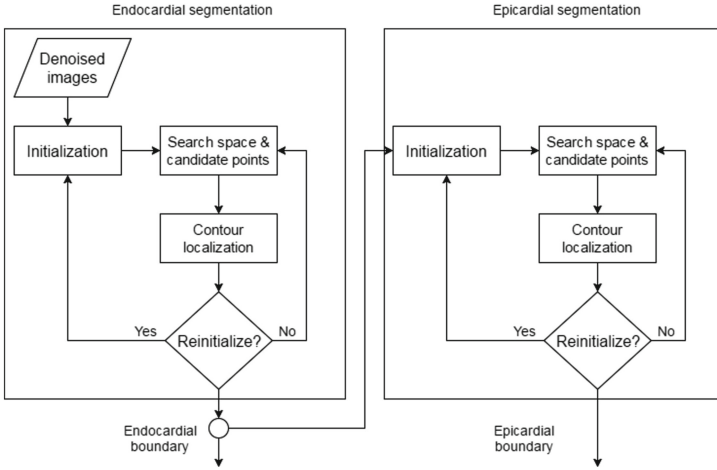


Fig. 1. Workflow of the algorithm

technique of Stable Principle Components Pursuit [10] which seeks an explicit noise component within the RPCA decomposition. If Y is the given matrix of dimensions $N_x N_y \times N_t$, then the method decomposes the matrix into a low-rank matrix L and a sparse matrix S by solving the following convex optimization problem.

$$\begin{aligned} \min_{L,S} \quad & \|L\| + \lambda_{sum} \|S\|_1 \\ \text{subject to} \quad & \|L + S - Y\|_F \leq \epsilon \end{aligned}$$

Here $\|\cdot\|_F$ is the Frobenius norm. The 1-norm $\|\cdot\|_1$ and the nuclear norm $\|\cdot\|$ are given by

$$\|S\|_1 = \sum_{(i,j)} \|S_{ij}\|, \|L\| = \sum_i \sigma_i(L)$$

and $\sigma_i(L)$ is the vector of singular values of L .

Physiologically, the low-rank part L appears as a static component while the sparse component S captures motion, in this particular case mostly heartbeats (Fig. 3(b) and (c)). The parameter λ_{sum} controls the relative importance of the low-rank term L vs. the sparse term S , and the parameter ϵ accounts for the unknown perturbations $Y - (L + S)$ in the data not explained by L and S . Higher the λ_{sum} value, faster the convergence rate and sparser the S matrix. The low rank approximation is seen to be robust to the value of λ_{sum} . We have taken $\lambda_{sum} = 0.1$ for the entire study. When $\epsilon = 0$, the SPCP reduces to the standard RPCA problem. ϵ is chosen to be a small value, as 0.05 times the norm of Y .

3.2 Grid Extraction from Tagged MR Images

To deal with ‘bleeding’ of the contour into the tags, the grid information is incorporated through an additional term in the cost function. The tags in one direction are extracted using a bandpass filter to isolate the spectral peak centered at the lowest harmonic frequency in the corresponding tag direction. The inverse fourier transform of the bandpass region returns a complex harmonic image comprising of a harmonic magnitude image and harmonic phase image. The harmonic phase image gives a detailed picture of the tags. Following edge extraction, a binary image G is obtained from the grid image such that a pixel on the grid and outside the grid gives values of 1 and 0 respectively (Fig. 2).

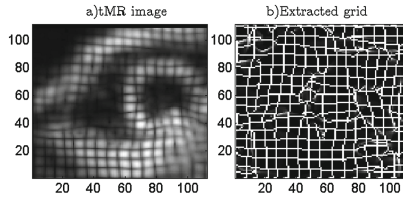


Fig. 2. Raw image (a) and the extracted grid (b)

3.3 Endocardial Segmentation

Initialization. If $N_x \times N_y$ are the dimensions of each image over N_t time points, SPCP is performed on the matrix of dimension $N_x N_y \times N_t$ following intensity homogenization to get a low rank image and sparse component. The low rank image approximates a ‘mean’ image across all timepoints. The low rank image is pre-processed (Fig. 3(d) and (e)) and an initial boundary is found from this image using intensity based Otsu’s method to separate the blood pool from heart walls. The largest non-boundary blob is then extracted to get an initial contour R_{init} for the endocardium.

Contour localization. The initial contour R^{init} is fit to a circle to approximate the ventricle. The circle is then sampled to get M points, $R_1, R_2, R_3 \dots R_M$, the number of points required in the final contour.

A search space is defined around each point, where it is allowed to move. A point is allowed to move perpendicular to the line joining the previous and next points in the contour. If the m^{th} point of the circular contour is R_m , the search space is defined as from $R_m - q$ to $R_m + q$, in the radial direction, where q is an appropriate search space size (See Fig. 4). To simplify the computation, we choose T points showing highest gradients in the defined direction. Lower T values result in noisier contours whereas higher values result in redundant

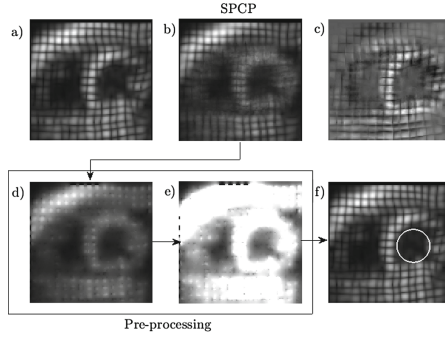


Fig. 3. (a) Original image. (b) Low rank image (c) Sparse image (d) Smoothed Low rank image (e) Histogram truncation (f) Initialized contour fitted into a circle

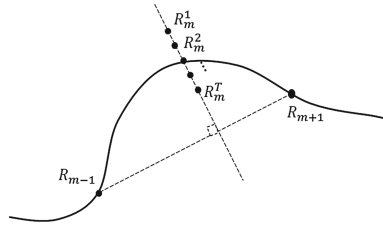


Fig. 4. T candidate points are found around R_{min} the direction perpendicular to the line joining R_{m-1} and R_{m+1}

information with longer computation time. In our case, we have taken $T = 5$ throughout the study.

DP is used to explore the search lists and find the optimal combination based on a cost function, which gives us the final contour R^f .

Cost function: For any endocardial candidate point p with indices (i, j) , three terms contribute to the cost associated with that point.

Gradient term: This energy term ensures that the contour is attracted to the edges.

$$F_1 = e^{-\lambda_1 \|\nabla_p I\|} \tag{1}$$

where $\|\nabla_p I\|$ represents the average magnitude of the gradient at point p in image I and its two neighbourhood slices. Using gradient information from three adjacent slices is found to improve robustness and accuracy and is a valid assumption due to thin slices. The grid penalty term described below is used to exclude high gradient terms arising in the tag regions.

Smoothness term: An approximate smoothness term is used,

$$F_2 = e^{-\lambda_2 * (\|p - C_0\| - \|p_0 - C_0\|)} \tag{2}$$

where p_0 is the point preceding the point p in the contour being found and C_0 is the centre of a circle fitted to initial endocardial boundary R^{init} . This term prevents any drastic changes in relative radii of points and consequently controls the curvature.

Grid penalty: A binary term is used to penalize pixel regions with the tags. The cost of a point p on tagged image with the corresponding grid image G is given by the indicator function

$$F_G = \chi_G(p) \quad (3)$$

F_G is 0 when the point being considered does not fall on any tags. The additional cost from the presence of a tag is $s_G F_G$, where s_G is the corresponding weight. The total cost associated with a point is therefore $s_1 F_1 + s_2 F_2 + s_G F_G$ where s_1 , s_2 and s_G are appropriate weights.

3.4 Epicardial Segmentation

Initialization. The delineated endocardial boundary R^f is used in initializing the epicardial boundary. At a point R_m^f on the endocardium, an intensity profile is considered radially and fit to a standard Gaussian. The standard deviation of the Gaussian is taken as the thickness th of the myocardial wall at that point. The corresponding point S_m in the initial epicardial contour is found by displacing R_m^f radially outwards by th to get the initial epicardial contour S^{init} .

Contour localization. S^{init} is fit to a circle and sampled to get N points $S_1, S_2, S_3 \dots S_N$ and search lists of size T are defined around every point. DP is used to explore the search lists and choose points from the candidate points. However a widely observed property of the epicardium is used to make a small modification to the cost function.

Cost function: Epicardial boundaries are often marked by a fall in intensity level, which in addition distinguishes the epicardial boundary from other boundaries nearby. To exploit this information an addition term is used, which we call the falling-edge term.

The falling-edge term at a point p is defined as the difference in directions of the gradient at that point and a ray through p , emanating from the centre. C_0 is the centre of a circle fitted to initial endocardial boundary R^{init} .

$$F_3 = |\angle \nabla_p I - \angle (C_0 - p)| \quad (4)$$

where \angle operator represents the direction. This term is zero when the gradient points to the centre and preferentially supports radially falling gradients. The total cost function for an epicardial point is then, $s_1 F_1 + s_2 F_2 + s_3 F_3 + s_G F_G$, where s_3 is the weight corresponding to F_3 . The contours found in one slice are used to propagate both spatially to segment the volume and then temporally to segment all phases of the cardiac cycle.

4 Contour Propagation

The contour initialization is done on an initial slice (mid ventricle) chosen from a volume acquired mid-diastole. Segmentation of the entire volume is done slice by slice. The contour on each slice is initialized using the final contour obtained on the adjacent slice. The final contour of the mid-ventricle slice is then transferred to the mid-ventricle slice of the volume acquired at a successive time point in the cardiac cycle and adjusted using DP (with appropriate cost functions described in the previous sections).

5 Results and Discussion

The algorithm is tested on database of tagged MR cardiac volumes of healthy individuals. Image volumes acquired throughout the cardiac cycle for all patients were segmented. The tMR images are noisy as they capture a single cardiac cycle for all patients. In spite of this, the algorithm gives good contour localization and propagation. Typical segmentation results propagated across the cardiac cycle as well as the volume are shown in Figs. 5 and 6 respectively. Apical slices give slightly less accurate segmentation results due to their difficulty in segmentation. The results are almost instantaneous due to the computational simplicity.

Propagating the contours sometimes result in the contours accumulating errors due to weak boundaries, noise, sudden geometry changes etc. This can be remedied by re-initialization of the contour. The algorithm also faces difficulty in providing accurate results at the apical slices. The cost function is

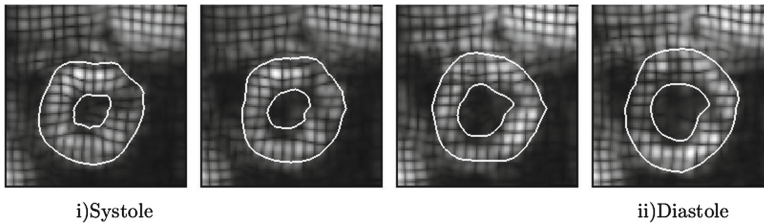


Fig. 5. Results of segmentation propagated across time

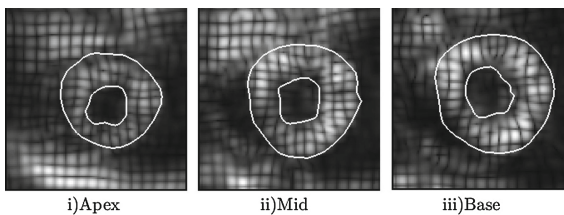


Fig. 6. Segmentation propagated across volume. Slices at apical, mid and basal level are shown

6 Conclusion

In this paper, we have presented a method to extract the contours of the myocardium in tagged MR cardiac volumes. Contour initialization is done using SPCP and propagated by minimizing (using DP) a cost function based on inherent image properties. It is able to successfully segment tagged MR images which pose serious challenges to traditional methods due to the presence of tags. The method is particularly suitable as a pre-processing step for cardiac deformation analysis & strain rate imaging.

References

1. Candès, E.J., Li, X., Ma, Y., Wright, J.: Robust principal component analysis? *J. ACM (JACM)* **58**(3), 11 (2011)
2. Edvardsen, T., Gerber, B.L., Garot, J., Bluemke, D.A., Lima, J.A., Smiseth, O.A.: Quantitative assessment of intrinsic regional myocardial deformation by doppler strain rate echocardiography in humans: validation against three-dimensional tagged magnetic resonance imaging. *Circulation* **106**(1), 50–56 (2002). doi:10.1161/01.CIR.0000019907.77526.75. <http://circ.ahajournals.org/content/106/1/50.abstract>
3. Guttman, M., Prince, J., McVeigh, E.: Tag and contour detection in tagged MR images of the left ventricle. *IEEE Trans. Med. Imaging* **13**(1), 74–88 (1994). doi:10.1109/42.276146. ISSN 0278-0062
4. Metaxas, D.N., Axel, L., Qian, Z., Huang, X.: A segmentation and tracking system for 4D cardiac tagged MR images, pp. 1541–1544 (2006)
5. Osman, N.F., Kerwin, W.S., McVeigh, E.R., Prince, J.L.: Cardiac motion tracking using CINE harmonic phase (HARP) magnetic resonance imaging. *Magn. Reson. Med. Official J. Soc. Magn. Reson. Med./Soc. Magn. Reson. Med.* **42**(6), 1048 (1999)
6. Qian, Z., Metaxas, D.N., Axel, L.: A learning framework for the automatic and accurate segmentation of cardiac tagged MRI images. In: Liu, Y., Jiang, T., Zhang, C. (eds.) CVBIA 2005. LNCS, vol. 3765, pp. 93–102. Springer, Heidelberg (2005). doi:10.1007/11569541_11
7. Tobon-Gomez, C., De Craene, M., Mcleod, K., Tautz, L., Shi, W., Hennemuth, A., Prakosa, A., Wang, H., Carr-White, G., Kapetanakis, S., et al.: Benchmarking framework for myocardial tracking and deformation algorithms: an open access database. *Med. Image Anal.* **17**(6), 632–648 (2013)
8. Yang, X., Murase, K.: Tagged cardiac MR image segmentation by contrast enhancement and texture analysis, pp. 4–210 (2009)
9. Zerhouni, E.A., Parish, D.M., Rogers, W.J., Yang, A., Shapiro, E.P.: Human heart: tagging with MR imaging—a method for noninvasive assessment of myocardial motion. *Radiology* **169**(1), 59–63 (1988). doi:10.1148/radiology.169.1.3420283. <http://dx.doi.org/10.1148/radiology.169.1.3420283>
10. Zhou, Z., Li, X., Wright, J., Candès, E., Ma, Y.: Stable principal component pursuit. In: *IEEE International Symposium on Information Theory Proceedings (ISIT)*, pp. 1518–1522. IEEE (2010)